Electronic Supporting Information

BiOCl with favorable surface state regulated by polyhydroxylated disaccharides for dramatically accelerated photodegradation capacity

Jintao Wang, [a] [1] Yuan Liu, [a] [1] Zhichen Wang, [b] Hao Mei, [b] Rongbin Zhang, *[a] and Xuewen Wang*[a]

[a]Key Laboratory of Jiangxi Province for Environment and Energy Catalysis, School of Chemistry and Chemical Engineering, Nanchang University, 999# Xuefu Road, Nanchang, 330031, China

[b]School of Future Technology, Nanchang University, 999# Xuefu Road, Nanchang, 330031, China

[1]These authors contribute equally to this work

Corresponding authors: Prof. Xuewen Wang, Prof. Rongbin Zhang

E-mail: wangxuewen@ncu.edu.cn; rbzhang@ncu.edu.cn

1.1 Characterization

The Fourier infrared spectrometer (FT-IR, Thermo Scientific Nicolet iS10) was employed for the detection of chemical bond vibrations and signals of functional groups in catalysts. The Scanning Electron Microscope (SEM, Hitachi, SU8100) was used for the morphological and structural characterizations. The X-ray powder diffraction (XRD, SmartLab9kw) was performed on a Rigaku diffractometer using Cu Kα radiation at a scanning speed of 30 º min^{-1} in the 2θ range of 5–80 º. The X-ray

photoelectron spectroscopy (XPS) was recorded on an X-ray photoelectron spectroscopy (XPS, ESCALAB-250Xi) with an Al Kα X-ray source, and the binding energy of all peaks was calibrated by the C 1s peak of adventitious carbon (284.6 eV). The UV−visible diffuse reflectance spectra (UV−vis DRS) were measured with a PerkinElmer Lambda 365 instrument using $BaSO_4$ powder as the reference sample. The time-resolved photo-luminescence (TRPL) spectra of electron quenching were carried by the Edinburgh steady-transient fluorescence spectrometer (FLS 1000). The specific surface areas of the samples were tested by the Brunauer-Emmett-Teller (BET, Kubo-X1000).

The electrochemical properties of the photocatalysts were measured by PARSTAT4000. The Mott-Schottky curves, LSV curves and electrochemical impedance spectroscopy (EIS) were carried out in a quartz three-electrode cell with catalysts coated on FTO, saturated Ag/AgCl electrode and platinum sheet as working, reference and counter electrode, respectively.

1.2 Photocatalytic Activity Measurement

The UV−vis light driven photocatalytic activity of all samples was evaluated by degrading 1×10^{-4} M methyl orange (MO), 1×10^{-3} M rhodamine B (Rh B), 100 mg/L tetracycline (TC), 10 mg/L ciprofloxacin (CIP) and 10 mg/L sulfamethoxazole (SMX). The 300 W short-arc xenon lamp (PLS-SXE 300+) was used as the light source. In a typical photocatalytic degradation experiment, 100 mg of the prepared composites were dispersed in 100 mL of an aqueous solution of MO, Rh B, TC, CIP and SMX, respectively. The mixture was stirred in the dark for 30 min before the light

irradiation to reach adsorption-desorption equilibrium. Later, the photocatalyst suspension was irradiated with a Xe lamp under stirring, and approximately 5 mL of the suspension was taken at intervals and centrifuged (9000 rpm for 10 min) to separate the photocatalyst from the solution. Eventually, the concentration of the remaining solution was measured using an UV−vis spectrophotometer (PerkinElmer Lambda 365).

Terephthalic acid (TPA) was chosen as a probe molecule to detect the formation of •OH on UV−vis irradiated BiOCl-H_2O, BiOCl-glucose and BiOCl-maltose. TPA can react with •OH to form a highly fluorescent compound called 2-hydroxy terephthalic acid (TAOH). Therefore, the amount of •OH can be determined by the PL intensity of TAOH at around 425 nm. Firstly, TPA was dissolved in NaOH aqueous solution to obtain a 1×10^{-4} M solution of TPA. Then, 100 mg of catalyst was added to 100 mL of TPA solution. The solution was ultrasonically dispersed and then adsorbed in the dark for 30 min. The solution was irradiated with a 300 W xenon lamp for 30 min. Finally, 5 mL of the solution was centrifuged at 9000 rpm for 10 min and PL measurements were obtained using a fluorescence spectrophotometer at an excitation wavelength of 315 nm.
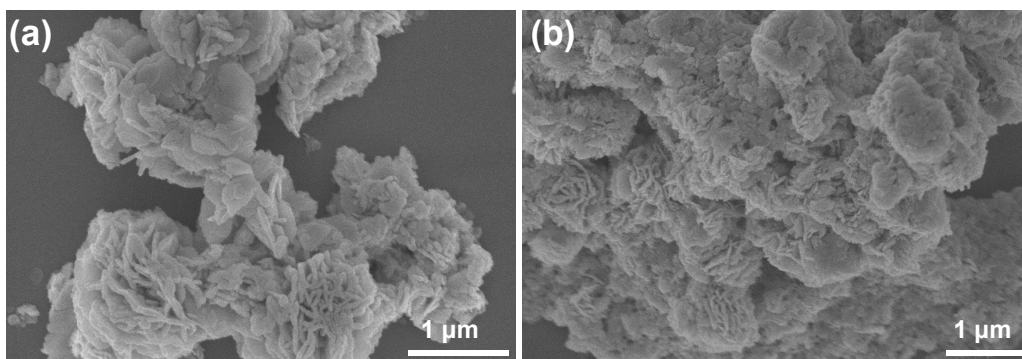
**Fig. S1** SEM images of BiOCl-sucrose (a) and BiOCl-lactose (b).
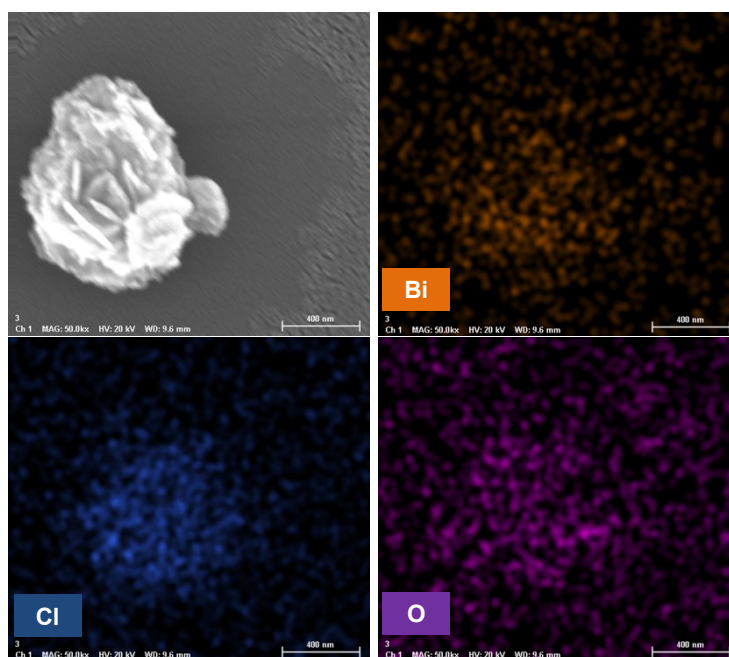
**Fig. S2** Elemental mapping of BiOCl-maltose.
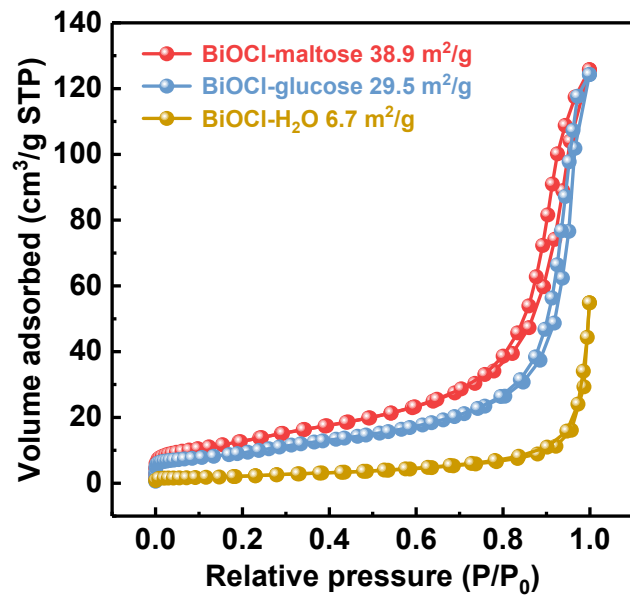
Fig. S3 N_2 adsorption-desorption isotherms of BiOCl-maltose, BiOCl-glucose and BiOCl-H_2O.

Table S1 Specific morphological information of BiOCl regulated by the single molecules that contain different numbers of hydroxyl groups.

| Modifiers	Number of hydroxyl groups	Morphology	BET area (m^2/g)
H_2O	0	nanosheet	6.7
Glucose	5	nanoflower	29.5
Maltose	8	nanoflower	38.9
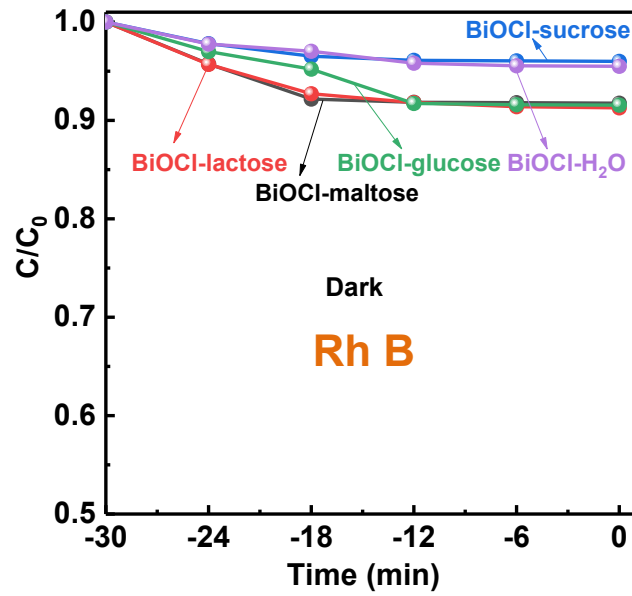
Fig. S4 Adsorption performance of BiOCl-maltose, BiOCl-sucrose, BiOCl-lactose, BiOCl-glucose and BiOCl-H$_2$O on Rh B in dark.
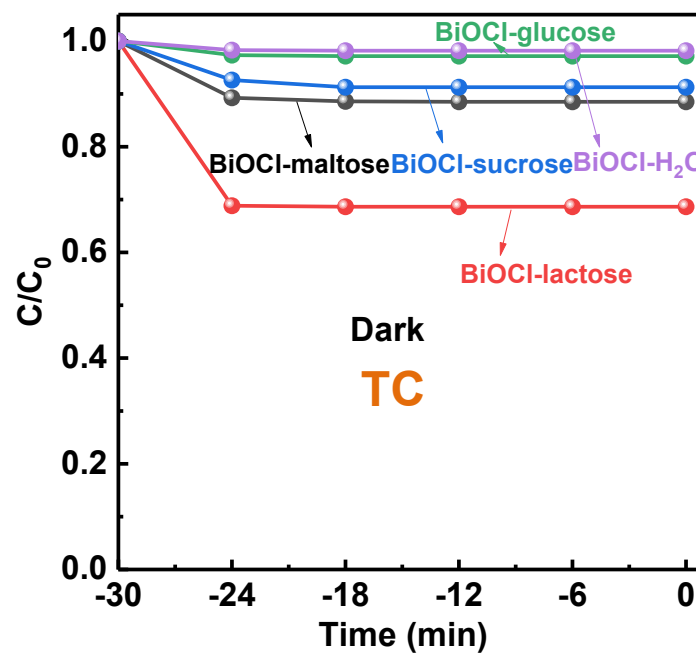
Fig. S5 Adsorption performance of BiOCl-maltose, BiOCl-sucrose, BiOCl-lactose, BiOCl-glucose and BiOCl-H$_2$O on TC in dark.
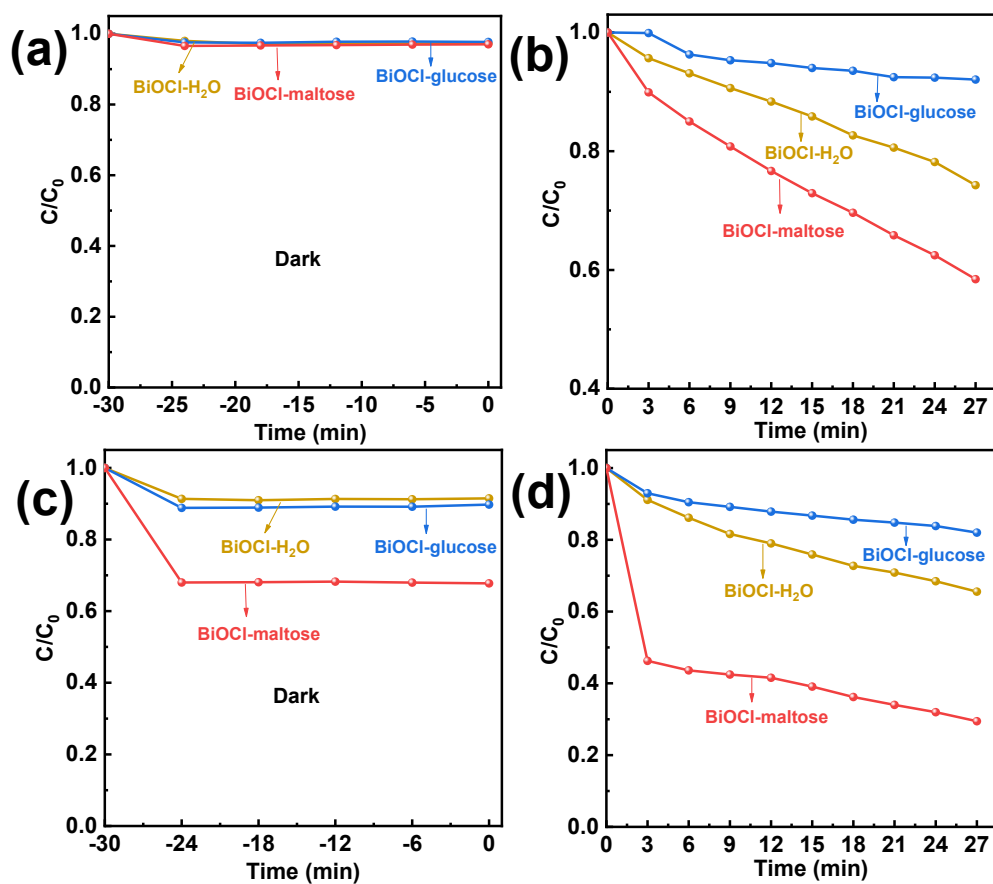
Fig. S6 (a) Adsorption performance in dark and (b) Photocatalytic degradation curve under UV−vis light of BiOCl-maltose, BiOCl-glucose, BiOCl-H$_2$O on SMX; (c) Adsorption properties in dark and (d) Photocatalytic degradation curves under UV−vis light of BiOCl-maltose, BiOCl-glucose, BiOCl-H$_2$O on CIP.

The process of catalyst-pollutant interaction and photocatalytic degradation mechanism are as follows:

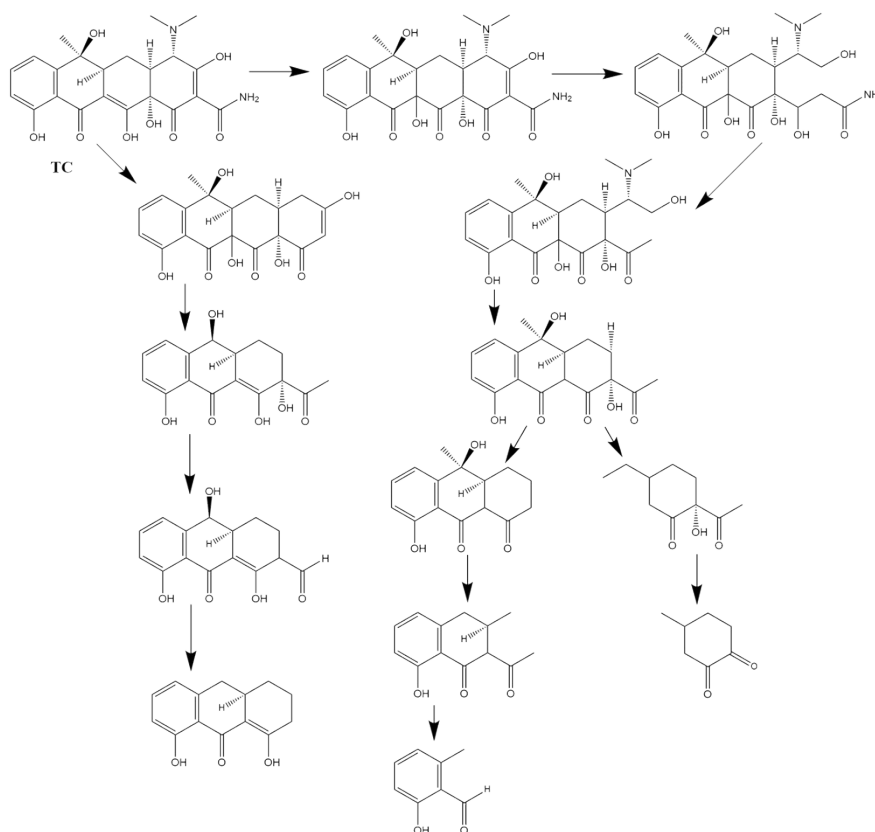i) Reaction equation for methyl orange (MO) degradation:[1]

$$MO + \cdot OH \rightarrow MO(HO\cdot) \rightarrow Intermediate + \cdot OH \rightarrow CO_2 + C_2O$$

Fig. S7 The possible degradation reaction process of MO.

ii) Rhodamine B (RhB) gradually dissociates 1-4 ethyl groups under the action of hydroxyl radicals, degradation reaction equation:[2-4]

$$RhB + hv(UV-vis\ light) \rightarrow RhB^*$$

$$RhB^* + \cdot OH \rightarrow RhB^{*-}$$

$$RhB^{*-} + \cdot OH \rightarrow CO_2 + H_2O + NO_3^-$$

iii) The possible degradation process of tetracycline (TC) is show in Fig. S8.[5-7]

Fig. S8 The possible degradation reaction process of TC.

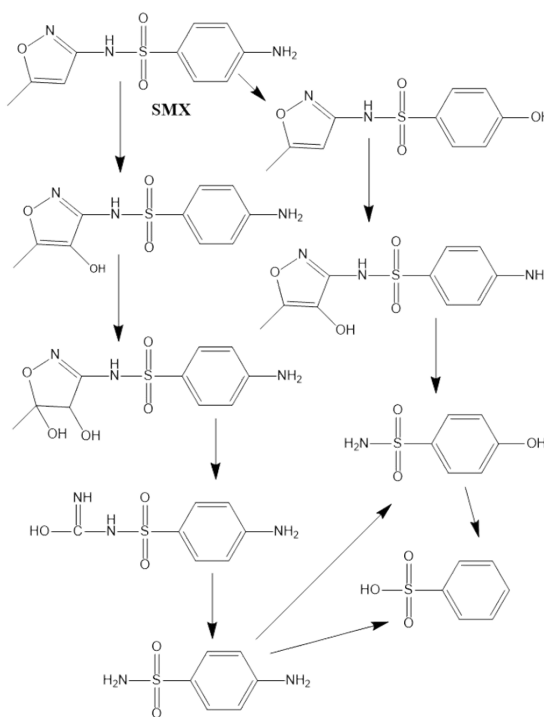iv) Sulfamethoxazole (SMX) can be degraded following equations:[8, 9]

Fig. S9 The possible degradation reaction process of SMX.

v) The possible degradation process of ciprofloxacin (CIP) is shown in Fig. S10.[10]
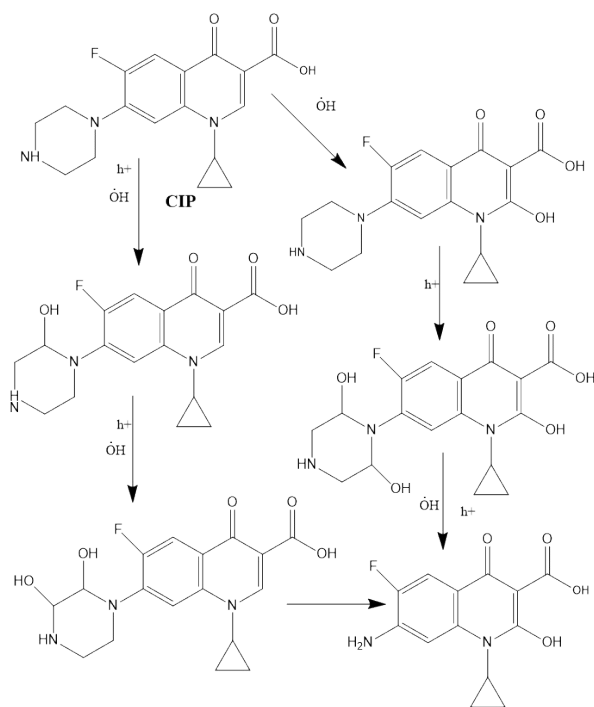

Fig. S10 The possible degradation reaction process of CIP.

Table S2 Degradation efficiencies of MO, Rh B and TC with BiOCl regulated by the single molecules containing different numbers of hydroxyl groups.

Modifiers	Number of hydroxyl groups	Degradation efficiency (MO)	Degradation efficiency (Rh B)	Degradation efficiency (TC)
H₂O	0	13.0%	3.5	45.5
Methanol	1	9.7	-	-
Ethanol	1	32.9	-	-
Ethylene glycol	2	4.1	-	-
Glycerol	3	8.9	-	-
Meso-erythritol	4	5.6	-	-
Glucose	5	17.0%	5.1	42.9
Maltose	8	91.5%	99.5	73.5
Sucrose	8	49.7%	99.6	63.1
Lactose	8	50.0%	98.4	65.5

References:

1. J. Han, H.-Y. Zeng, S. Xu, C.-R. Chen and X.-J. Liu, *Appl. Catal. A-Gen.*, 2016,

527, 72-80.

2.   M. Sundararajan, V. Sailaja, L. John Kennedy and J. Judith Vijaya, *Ceram Int.*, 2017, **43**, 540-548.

3.   J. Xie, Y. Cao, D. Jia and Y. Li, *J Colloid Interf Sci.*, 2017, **503**, 115-123.

4.   L. Zhang, Y. Meng, H. Shen, J. Li, C. Yang, B. Xie and S. Xia, *Appl. Surf. Sci.*, 2021, **567**, 150760.

5.   S. Li and J. Hu, *J Hazard Mater.*, 2016, **318**, 134-144.

6.   H. Liu, W. Huo, T. C. Zhang, L. Ouyang and S. Yuan, *Mater. Today Chem.*, 2022, **23**, 100729.

7.   M. Lu, M. Liu, Y. Wei, H. Xie, W. Fan, J. Huang, J. Hu, P. Wei, W. Zhang, Y. Xie and Y. Qi, *J Alloy Compd.*, 2023, **936**, 168273.

8.   Z. Cheng, Z. Zuo, S. Yang, Z. Yuan, X. Huang and Y. Liu, *Water Res.*, 2021, **189**, 116629.

9.   H. Gong and W. Chu, *J Hazard Mater.*, 2016, **314**, 197-203.

10. X. Hu, X. Hu, Q. Peng, L. Zhou, X. Tan, L. Jiang, C. Tang, H. Wang, S. Liu, Y. Wang and Z. Ning, *Chem Eng J.*, 2020, **380**, 122366.